THE JOURNAL OF BIOLOGICAL CHEMISTRY VOL. 283, NO. 18, pp. 12284–12292, May 2, 2008

Highly Conserved Asparagine 82 Controls the Interaction of Na^+ with the Sodium-coupled Neutral Amino Acid Transporter SNAT2*[S]

Received for publication, August 14, 2007, and in revised form, March 3, 2008 Published, JBC Papers in Press, March 4, 2008, DOI 10.1074/jbc.M706774200

Zhou Zhang[‡§], Armanda Gameiro[‡¶], and Christof Grewer[‡¶1]

From the [‡]Department of Physiology and Biophysics, University of Miami School of Medicine, Miami, Florida 33136, the [¶]Department of Chemistry, Binghamton University, Binghamton, New York 13902, and the [§]College of Life and Environment Sciences, Shanghai Normal University, 100 Guilin Road, Shanghai 200234, China

The neutral amino acid transporter 2 (SNAT2), which belongs to the SLC38 family of solute transporters, couples the transport of amino acid to the cotransport of one Na^+ ion into the cell. Several polar amino acids are highly conserved within the SLC38 family. Here, we mutated three of these conserved amino acids, Asn^{82} in the predicted transmembrane domain 1 (TMD1), Tyr^{337} in TMD7, and Arg^{374} in TMD8; and we studied the functional consequences of these modifications. The mutation of N82A virtually eliminated the alanine-induced transport current, as well as amino acid uptake by SNAT2. In contrast, the mutations Y337A and R374Q did not abolish amino acid transport. The K_m of SNAT2 for its interaction with Na^+, K_{Na^+}, was dramatically reduced by the N82A mutation, whereas the more conservative mutation N82S resulted in a K_{Na^+} that was in between $SNAT2_{N82A}$ and $SNAT2_{WT}$. These results were interpreted as a reduction of Na^+ affinity caused by the Asn^{82} mutations, suggesting that these mutations interfere with the interaction of SNAT2 with the sodium ion. As a consequence of this dramatic reduction in Na^+ affinity, the apparent K_m of $SNAT2_{N82A}$ for alanine was increased 27-fold compared with that of $SNAT2_{WT}$. Our results demonstrate a direct or indirect involvement of Asn^{82} in Na^+ coordination by SNAT2. Therefore, we predict that TMD1 is crucial for the function of SLC38 transporters and that of related families.

Transporters for small, neutral amino acids are essential for the shuttling of glutamine, the major nitrogen carrier in mammalian organisms, into and out of cells (1–3). Recently, a number of genes belonging to a family of sodium-coupled neutral amino acid transporters (SNAT[2]; SLC38 gene family) have been cloned (4–11). The SLC38 gene family has six known members. Member 2 of the family, SNAT2, is widely expressed is mammalian tissue (12, 13), and its functional properties match those of the classically assigned system A transporters (5, 6, 12, 14–16). Although amino acid transport by SNATs is important for the physiological function of many tissues, it plays a particularly critical role in the brain (17), where it is believed to help shuttle glutamine from astrocytes to neurons via the glutamate-glutamine cycle. This process is essential for recycling the neurotransmitter glutamate.

Transport of neutral amino acids by SNAT2 is coupled to the cotransport of Na^+ ions, with a proposed coupling stoichiometry of 1 neutral amino acid to 1 Na^+ ion (14, 18, 19). Although the amino acid is a neutral zwitterion, the Na^+ ion carries charge. Therefore, it is possible that charged residues in the transmembrane domain of SNAT2 contribute to transport by counterbalancing charge on the substrate/Na^+ ion. However, the transmembrane domains (TMDs) of SNAT2 predicted from hydropathy analysis contain only two charged residues, one of which (His^{304}) did not significantly affect the kinetics of Na^+ binding to SNAT2 upon mutation to alanine (20). In addition to charged residues, amino acids with polar side chains often interact with Na^+ ions or charged groups of the amino acid in other Na^+-coupled amino acid transporters, of which bacterial homologues have been crystallized (21, 22). In any case, it is not known whether amino acids with polar or charged side chains contribute to Na^+ and/or substrate binding of SNAT2 and whether they are required for amino acid transport.

Here, we have modified by mutagenesis the amino acid residues Asn^{82}, Tyr^{337}, and Arg^{374}, which are highly conserved throughout the mammalian SLC38 members and also some fungal members of the superfamily. Asn^{82} is localized in the predicted TMD1 (Fig. 1*A*), in which 87.5% of residues are conserved within the SLC38 transporters, suggesting that TMD1 may be very important for the function of SNAT2. When asparagine 82 was mutated to alanine (N82A) or serine (N82S), the mutant transporters mediated only small transport current and no significant amino acid uptake, whereas the Y337A and R374Q mutations had less effect on amino acid transport. Determination of the effect of Na^+ on transport currents showed that the affinities for Na^+ and, consequently, alanine were dramatically affected by the N82A mutation, whereas the more conservative mutation N82S resulted in affinities for both alanine and Na^+ that were in between $SNAT2_{N82A}$ and $SNAT2_{WT}$. Together, our results demonstrate that mutations

* This work was supported by Florida Department of Health Grant 04NIR-07 and National Institutes of Health Grant R01-NS049335-02 (to C. G.). The costs of publication of this article were defrayed in part by the payment of page charges. This article must therefore be hereby marked "*advertisement*" in accordance with 18 U.S.C. Section 1734 solely to indicate this fact.

[S] The on-line version of this article (available at http://www.jbc.org) contains supplemental Figs. S1–S4.

[1] To whom correspondence should be addressed: Dept. of Chemistry, Binghamton University, 4400 Vestal Pkwy. E., Binghamton, NY 13902. Tel.: 607-777-3250; Fax: 607-777-4478; E-mail: cgrewer@binghamton.edu.

[2] The abbreviations used are: SNAT, sodium-coupled amino acid transporter; SLC, solute carrier; TMD, transmembrane domain; PBS, phosphate-buffered saline; Mes, methanesulfonate; MeAIB, α-methylamino-isobutyric acid; Glu, gluconate; HEK, human embryonic kidney; ANOVA, analysis of variance.

to position 82 interfere with Na^+ activation of amino acid transport by SNAT2, suggesting a direct or indirect involvement of Asn^{82} in Na^+ coordination by SNAT2.

EXPERIMENTAL PROCEDURES

Molecular Biology and Transient Expression—The cDNA coding for rat SNAT2, which was kindly provided by H. Varoqui, was subcloned into the SacI and NheI sites of a modified pBK-CMV vector (Δ(1098–1300)) (Stratagene), containing the cytomegalovirus promoter for mammalian expression. Wild-type SNAT2 was used for site-directed mutagenesis according to the QuikChange protocol (Stratagene, La Jolla, CA), as described by the supplier. The primers for mutation experiments were obtained from the DNA core lab of the Department of Biochemistry at the University of Miami School of Medicine. The complete coding sequences of mutated SNAT2 clones were subsequently sequenced. Wild-type and mutant transporter constructs were used for transient transfection of subconfluent human embryonic kidney cell (HEK293T/17, ATCC number CRL 11268) cultures using FuGENE 6 transfection reagent (Roche Applied Sciences) according to the instructions of the supplier. Electrophysiological recordings were performed between days 1 and 3 post-transfection.

Immunohistochemistry—Immunostaining to test for expression of mutant SNAT2 was performed as follows. Non-transfected or transfected HEK293 cells plated on poly(D-lysine)-coated coverslips were washed two times with phosphate-buffered saline (PBS) and then fixed in 3% (w/v) paraformaldehyde in PBS for 25 min at room temperature. After several washing steps with PBS, the cells were permeabilized with 0.1% (v/v) Triton X-100 in PBS at room temperature for 10 min. After a washing step with PBS, they were blocked with 0.2% (w/v) bovine serum albumin in PBS for 30 min at room temperature and then incubated with 0.005 mg/ml affinity-purified SNAT2 antibody (synthesized by Bethyl Laboratories. Inc.) in 0.5% (w/v) bovine serum albumin and 0.1% (v/v) Triton X-100 in PBS for 1 h at room temperature. This antibody was raised against a portion of the N terminus of SNAT2, which is located in the cytoplasm. Following primary antibody incubation, the cells were rinsed and incubated for 1 h with anti-rabbit IgG conjugated to Cy3 (1:500; Dianova) in PBS containing 0.5% (w/v) bovine serum albumin and 0.1% (v/v) Triton X-100. After being washed with PBS and water, the cells were mounted with antifade reagent (Molecular Probes) and stored in the dark. The Cy3 immunofluorescence was excited with a mercury lamp, visualized with an inverted microscope (Zeiss) by using a TMR filter set (Omega), and photographed with a digital camera (Canon).

Amino Acid Uptake Assay—HEK293 cells were plated on collagen-coated 12-well dishes (1×10^5 cells/well) in Dulbecco's modified Eagle's medium containing 10% fetal bovine serum, penicillin (100 units/ml), streptomycin (100 mg/ml), and glutamine (4 mM). 48 h after transfection with vector, wild-type SNAT2, or mutant transporter cDNA, the cells were washed with uptake buffer two times. The uptake buffer contained 140 mM sodium methanesulfonate (NaMes), 2 mM $MgMes_2$, 2 mM calcium gluconate ($CaGlu_2$), 30 mM TrisMes, pH 8.0, 5 mM glucose. The cells were then preincubated in the same buffer for 5 min at 37 °C before the buffer was removed and replaced with fresh buffer containing unlabeled α-methylamino-isobutyric acid (MeAIB) and 0.4 μCi of [^{14}C]MeAIB (PerkinElmer Life Sciences; total concentration, 40 μM). After 1 min of incubation at room temperature, uptake was terminated by washing twice with 1 ml of uptake buffer on ice (after 1 min uptake was in the linear range, as determined by quantifying the time dependence of uptake for times up to 5 min). The cells were then solubilized in 0.5 ml of 1% SDS, and radioactivity was measured by scintillation counting in 3 ml of scintillation fluid. The MeAIB uptake measurements were performed in duplicate.

Electrophysiology—SNAT2-mediated currents were recorded with an Adams & List EPC7 amplifier under voltage clamp conditions in the whole cell current recording configuration. The typical resistance of the recording electrode was 2–3 MΩ; the series resistance was 5–8 MΩ. Because the currents induced by substrate, anion, or cation application were small (typically, <200 pA), series resistance (R_S) compensation had a negligible effect on the magnitude of the observed currents (<4% error). Therefore, R_S was not compensated. The extracellular bath buffer solution contained 140 mM sodium methanesulfonate (NaMes), 2 mM magnesium gluconate ($MgGlu_2$), 2 mM calcium gluconate ($CaGlu_2$), 30 mM Tris, pH 8.0. All of the experiments were conducted at extracellular pH of 8.0 because amino acid transport by SNAT2 is pH-dependent, and the transport rate is maximal at pH 8.0. Under the experimental conditions used in our experiments, alanine is not expected to accumulate in the cytosol to concentrations higher than a few μM. Thus, no *trans*-inhibition should occur, even after long exposure of the cells to alanine. For testing the [Na^+] dependence of the currents, Na^+ in the extracellular solution was replaced with *N*-methylglucamine. The pipette solution contained 140 mM KSCN, 2 mM $MgGlu_2$, 10 mM EGTA, 10 mM HEPES, pH 7.3. For determining the voltage dependence of SNAT2 alanine transport, a combined voltage ramp/solution exchange protocol was used. In this protocol, the cell membrane was initially held at 0 mV before ramping the voltage to its final value (−150 to +90 mV) within 2 s. 2 s after establishing the new voltage, the extracellular solution was changed from no alanine to the final concentration of alanine, followed by ramping the voltage back to 0 mV. The currents were low pass filtered at 1–10 kHz (Krohn-Hite 3200) and digitized with a digitizer board (Axon, Digidata 1200) at a sampling rate of 10–50 kHz, which was controlled by software (Axon PClamp). All of the experiments were performed at room temperature.

Rapid Solution Exchange—Rapid solution exchange was performed as described previously (23). Briefly, substrates were applied to a voltage-clamped, SNAT2-expressing cell suspended at the tip of the current recording electrode by means of a quartz tube (opening diameter, 350 μm) positioned at a distance of ~0.5 mm to the cell. The linear flow rate of the solutions emerging from the opening of the tube was ~5–10 cm/s, resulting in typical rise times of the whole cell current of 30–50 ms (10–90%).

Data Analysis—Nonlinear regression fits of experimental data were performed with Origin (Microcal Software, Northampton, MA) or Clampfit (pClamp8 software; Axon Instruments, Foster City, CA). Dose-response relationships of cur-

rents were fitted with a Michaelis-Menten-like equation, yielding K_m and I_{max}. Endogenous electrogenic alanine transport activity in HEK293T cells, as measured by current recording from nontransfected cells, is minimal (see "Results"). For the [Na^+] dependence of the leak current, the dose-response data were corrected by subtraction of the nonspecific component of the current, which increased linearly with increasing [Na^+]. The nonspecific component was determined from nontransfected HEK293 cells. Each experiment was repeated at least three times with at least two different cells. The *error bars* represent the means ± S.D., unless stated otherwise. Maximum SNAT2-dependent currents, I_{max}, vary approximately by a factor 3 between different cells, depending on the expression levels of each individual cell. Such changes in expression levels did not affect the K_m for the amino acid. The I_{max} values were obtained by averaging the I_{max} values from these individual cells.

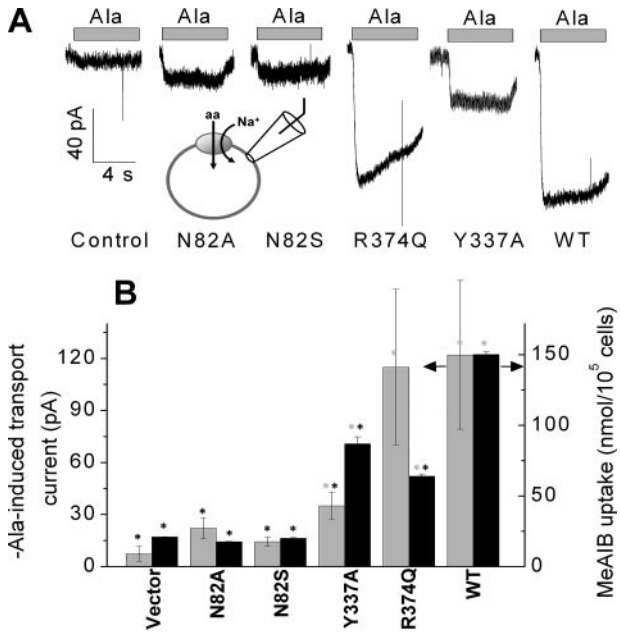

FIGURE 1. **Mutations to position 82 inhibit alanine transport currents and amino acid uptake.** *A*, typical transport currents induced by application of 10 mM alanine to nontransfected (control) and $SNAT2_{N82A}$-, $SNAT2_{N82S}$-, $SNAT2_{R374Q}$-, $SNAT2_{Y337A}$-, and $SNAT2_{WT}$-expressing cells. The bath solution contained 140 mM NaMes, and the pipette solution contained 140 mM KMes at 0 mV transmembrane potential. *B*, average alanine-induced transport currents (*gray bars*, *left axis*) and MeAIB uptake (*black bars*, *right axis*) in HEK293 cells transiently transfected with vector (pBK-CMV (Δ(1098–1300)), mutant transporter, and wild-type (*WT*) cDNA. Transport of [^{14}C]MeAIB (40 μM) was measured at 1 min in NaMes-containing buffer. The leak currents were subtracted. The large *error bar* of the currents in the $SNAT2_{WT}$-expressing cells is caused by the up to 3-fold differences in expression levels between different cells. The *black asterisks* indicate statistical significance compared with $SNAT2_{WT}$ at the $p < 0.05$ level, as determined by one-way ANOVA followed by Tukey's post-hoc analysis. Statistical significance *versus* control currents/uptake is illustrated by the *gray asterisks*.

RESULTS

Amino Acid Transport Is Impaired by Mutations to Position Asn^{82}—Application of 10 mM L-alanine to voltage-clamped, $SNAT2_{WT}$-expressing HEK293 cells resulted in inwardly directed whole cell currents (typical trace shown in Fig. 1*A*) in the presence of Na^+ at the extracellular side of the membrane ($V = 0$ mV, average current of −122 ± 40 pA, $n = 7$; *gray bars* in Fig. 1*B*). This inward current returned to the base line without considerable overshoot after removal of alanine (supplemental Fig. S1). In contrast, application of 10 mM alanine to SNAT2 with the mutation N82A or the more conservative N82S mutation resulted in small inward currents (Fig. 1*A*), which were on average 12 ± 5 and 6 ± 3% of the $SNAT2_{WT}$ response, respectively (corrected for nonspecific currents; Fig. 1*B*). These inward currents in $SNAT2_{N82A}$, although statistically not significantly larger than control currents at 0 mV, were caused by residual electrogenic transport of alanine, as demonstrated in supplemental Fig. S2 (see also results at −30 to −90 mV, which show inward currents significantly larger than control; Fig. 3*C*). These results suggest that mutations in position 82 strongly interfere with the ability of SNAT2 to catalyze alanine transport current. Although it is possible that the lack of current activity of $SNAT2_{N82A}$ is caused by a heterogeneous population of transporters with one population that is fully inactive and another small population that has wild-type-like activity, this scenario is unlikely because we do not see any evidence for a heterogeneous population of transporters in our data, such as dose-response curves (Fig. 2). Furthermore, if a small, fully active fraction would be responsible for the residual transport current, then it is expected that this fraction has functional properties similar to those of the wild-type, fully active form. However, the experimental data contradict this expectation, showing that K_m values for Na^+ and substrate are dramatically changed compared with those of the wild-type transporter (Fig. 2).

In contrast to mutations in position 82, the mutation R374Q did not significantly affect the alanine-induced transport current, whereas the Y337A mutation impaired transport current, but not to the same degree as the N82 mutations (Fig. 1*B*). Nontransfected HEK293 cells showed only little response to 10 mM alanine (−7 ± 4 pA, $n = 8$; Figs. 1*A* and *B*).

The lack of alanine-induced transport current in the Asn^{82} mutant transporters may be caused by reduced expression. To test this possibility, we performed immunostaining experiments with a primary antibody recognizing the intracellular N terminus of SNAT2 in perme-

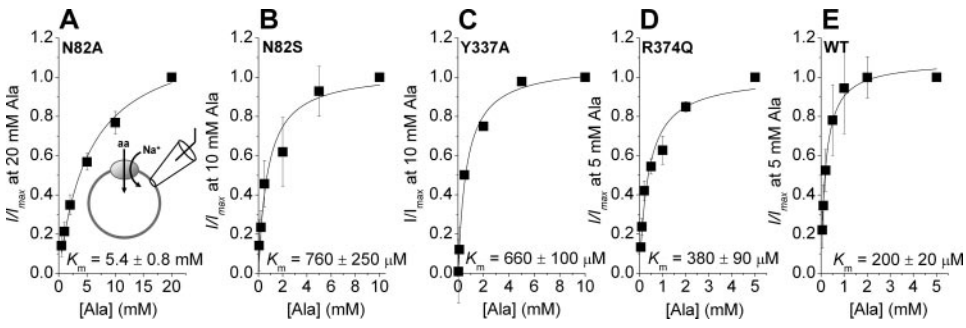

FIGURE 2. **Mutations in position 82 reduce the apparent amino acid affinity.** Apparent affinities for the substrate L-alanine of $SNAT2_{N82A}$ (*A*), $SNAT2_{N82S}$ (*B*), $SNAT2_{Y337A}$ (*C*), $SNAT2_{R374Q}$ (*D*), and $SNAT2_{WT}$ (*E*) were determined by recording substrate-induced transport current as a function of [alanine] at 0 mV. The bath solution contained 140 mM NaMes, and the pipette solution contained 140 mM KMes.

abilized cells (supplemental Fig. S3). Nontransfected cells showed no significant immunofluorescence, whereas $SNAT2_{WT}$-expressing cells were immunostained, showing intracellular labeling, but also fluorescence at the cell boundaries. This result is consistent with the membranous localization of SNAT2 observed in the electrophysiological recordings. This expression pattern of the transporter was not significantly changed in $SNAT2_{N82A}$ and $SNAT2_{N82S}$, which also showed staining at the cell boundaries. Although diffraction-limited visible light fluorescence microscopy does not allow us to directly differentiate whether the transporters are localized in the membrane or very close to the membrane, the unchanged N82A immunostaining pattern together with the existence of alanine-induced currents suggest that the mutant transporter is, in fact, localized in the membrane. This conclusion is also in agreement with recently published data on the related system N transporter SNAT3 with the analogous mutation N76H, which was shown to be expressed in the membrane (24).

To test whether the lack of alanine-induced transport current in $SNAT2_{N82A}$ and $SNAT2_{N82S}$ is caused by a loss of transport activity or by reduced electrogenicity of amino acid transport, we performed amino acid uptake experiments. Whereas wild-type transfected cells showed significant specific MeAIB uptake activity (7-fold higher than vector-transfected control cells), specific uptake was insignificant in $SNAT2_{N82A}$ and $SNAT2_{N82S}$-transfected cells (Fig. 1*B*). These results support the electrophysiological analysis of these mutant transporters, indicating that the Asn^{82} mutations result in a loss of transport as well as uptake activity. Although the R374Q and Y337A mutations also resulted in some loss of MeAIB uptake activity (43 ± 1 and 58 ± 1% of wild-type control, respectively; Fig. 1*B*), this loss was not as dramatic as that seen for the Asn^{82} mutations.

The loss of alanine transport activity of the mutant transporters may be caused by an increased K_m for alanine. To test this possibility, we performed kinetic analysis of alanine-induced transport currents, which showed that the K_m of $SNAT2_{N82A}$ for alanine was reduced dramatically compared with the wild-type transporter (V = 0 mV; Fig. 2*A* and Table 1). The apparent K_m of $SNAT2_{N82A}$ for alanine was 5.4 ± 0.8 mM ($n = 8$), which represents a 27-fold increase compared with that of $SNAT2_{WT}$ ($K_m = 200 \pm 20$ μM, $n = 5$; Fig. 2*E* and Table 1). The more conservative mutation N82S resulted in a K_m for alanine in between the wild-type and N82A transporters ($K_m = 760 \pm 250$ μM, $n = 5$; Fig. 2*B* and Table 1; but note that transport current is larger for $SNAT2_{N82A}$), which only increased by 3.5-fold compared with wild-type SNAT2. In contrast to the Asn^{82} mutations, the R374Q and Y337A mutations had a smaller effect on the K_m for alanine, with K_m increases of 2–3-fold, which were not statistically significant (Table 1 and Fig. 2, *C* and *D*).

Because $SNAT2_{N82A}$ and $SNAT2_{N82S}$ catalyzed very small alanine-induced transport currents at 0 mV (Fig. 1*B*), we determined the K_m of $SNAT2N_{82A}$ and $SNAT2_{N82S}$ for alanine also at −60 mV (summarized in Table 1), to get more accurate results. At this potential, the K_m values of $SNAT2_{N82A}$ and $SNAT2_{N82S}$ for alanine were 4.4 ± 0.5 mM ($n = 4$) and 460 ± 90 μM ($n = 5$), respectively. The K_m value of $SNAT2_{WT}$ for alanine was 120 ± 4 μM at −60 mV ($n = 4$). Statistical analysis indicated that the voltage dependence of the K_m values of the mutant transporters was not significant (Table 1, legend). However, consistent with the data obtained at 0 mV, these results suggest that mutations to position 82, but not to Arg^{374} and Tyr^{337} dramatically reduce transport activity and increase the K_m of SNAT2 for the substrate. Therefore, the following analyses will focus mainly on the Asn^{82} mutations.

TABLE 1

K_m for Ala to $SNAT2_{WT}$ and SNAT2 mutant transporters at different membrane potentials (140 mM intracellular K_m values)

Two-way ANOVA indicates no significant difference between the groups at 0 and −60 mV. ND, not detected.

	Membrane potential	
	0 mV	−60 mV
	μM	
$SNAT2_{WT}$	200 ± 20	120 ± 4
$SNAT2_{N82A}$	5400 ± 800[a]	4400 ± 500[a]
$SNAT2_{N82S}$	760 ± 250[a]	460 ± 90[a]
$SNAT2_{Y337A}$	660 ± 100	ND
$SNAT2_{R374Q}$	380 ± 90	ND

[a] Significantly altered K_m for the transporters with the mutations N82A and N82S compared with wild-type at the $p < 0.05$ level, as determined by one-way ANOVA within each membrane potential group, followed by Tukey's post-hoc analysis.

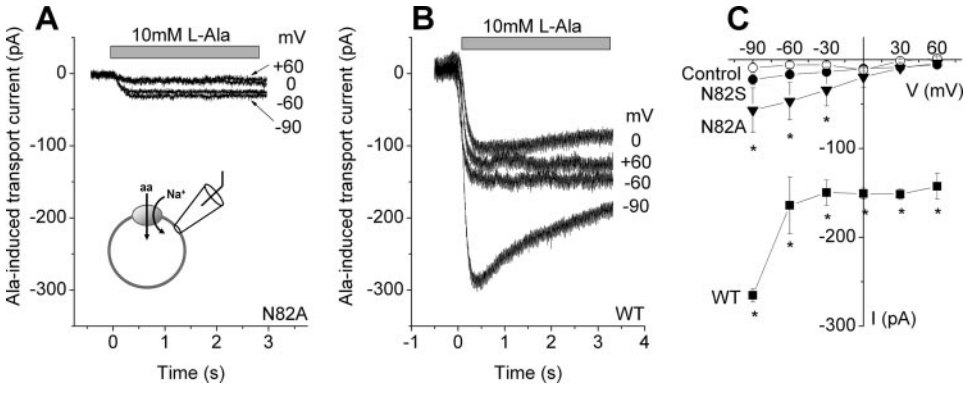

FIGURE 3. **Voltage dependence of L-alanine-induced transport currents at a concentration of 10 mM for $SNAT2_{N82A}$ (*A*) and $SNAT2_{WT}$ (*B*).** *C*, average current-voltage relationships of alanine-induced transport currents in nontransfected cells (control, *open circles*) as well as $SNAT2_{N82A}$- (*solid triangles*), $SNAT2_{N82S}$- (*closed circles*), and $SNAT2_{WT}$-expressing cells (*solid squares*). Statistical significance over control (one-way ANOVA within each membrane potential group followed by Tukey's post-hoc analysis) is indicated by the *asterisks* ($p <$ 0.05 level). Two-way ANOVA indicates significant difference between the WT, N82A, and control groups. *WT*, wild type.

To test whether transport activity of the Asn^{82} mutant SNAT2s can be restored by an increase in the electrical driving force, we determined the voltage dependence of alanine-induced transport currents. L-Alanine evoked inward transport currents in $SNAT2_{WT}$ (measured 4 s after alanine application and at saturating concentration of amino acid) showed a relatively small dependence on the membrane potential from −60 mV to +60 mV but increased steeply at a potential of −90 mV (1.75 times the current at 0 mV; Fig. 3, *B* and *C*). This steep increase may be caused by a slow,

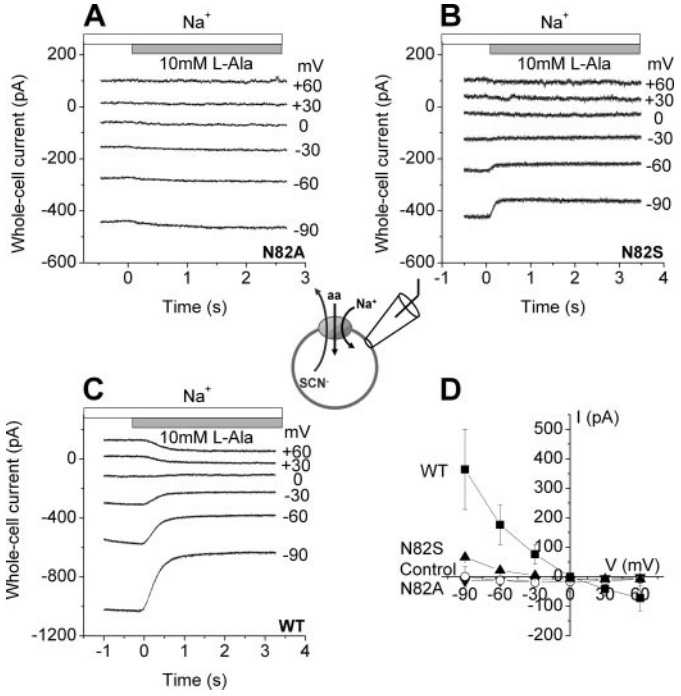

FIGURE 4. **Mutations in position 82 inhibit the alanine-sensitive anion leak conductance of SNAT2.** Voltage dependence of alanine-sensitive currents mediated by $SNAT2_{N82A}$ (*A*), $SNAT2_{N82S}$ (*B*), and $SNAT2_{WT}$, adapted from Ref. 20 (*C*), in the presence of 140 mM intracellular KSCN and 140 mM extracellular NaMes. 10 mM L-alanine was applied at $t = 0$ s, as indicated by the *bar*. *D*, current-voltage relationships of L-alanine-sensitive currents (10 mM) in nontransfected cells (*open circles*) and $SNAT2_{N82A}$- (*down triangles*), $SNAT2_{N82S}$- (*up triangles*), and $SNAT2_{WT}$- (*squares*) expressing cells in the presence of 140 mM intracellular SCN^-. *WT*, wild type.

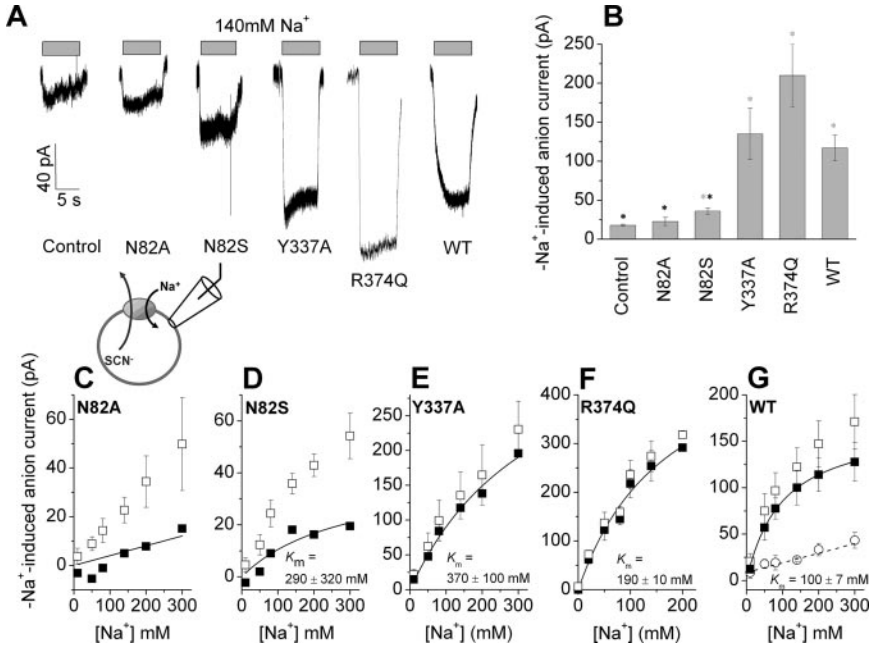

FIGURE 5. **Mutations in position 82 inhibit Na^+-dependent anion leak currents and interfere with Na^+ interaction with SNAT2.** Whole cell current recordings were performed with a KSCN-based pipette solution (140 mM) and at 0 mV transmembrane potential. *A*, comparison of typical leak anion currents induced by the application of 140 mM extracellular Na^+ between nontransfected cells (control), cells expressing mutant, and wild-type SNAT2 (Na^+ application indicated by the *gray bars*). *B*, statistical analysis of average Na^+-induced anion currents. The *black asterisks* indicate statistical significance compared with $SNAT2_{WT}$ at the $p < 0.05$ level, as determined by one-way ANOVA followed by Tukey's post-hoc analysis. Statistical significance *versus* control currents is illustrated by the *gray asterisk*. Leak anion currents as a function of extracellular $[Na^+]$ for $SNAT2_{N82A}$ (*C*), $SNAT2_{N82S}$ (*D*), $SNAT2_{Y337A}$ (*E*), $SNAT2_{R374Q}$ (*F*), and $SNAT_{WT}$ (*G*) (*solid squares*, after subtracting the nonspecific currents; *open circles*, determined from nontransfected cells). The *open squares* in *C*--*F* indicate results from the original experiments before subtraction of the nonspecific leak currents (*open circles*) determined in nontransfected control cells. *WT*, wild type.

voltage-dependent inactivation process, which is most prevalent at negative voltages, because it is not seen in I-V relationships obtained 20 ms after a voltage jump (data not shown). Alanine-induced (10 mM) transport currents mediated by $SNAT2_{N82A}$, although small compared with $SNAT2_{WT}$, increased with increasingly negative membrane potential with a steeper voltage dependence (three times in a 90-mV voltage range; Fig. 3, *A* and *C*), indicating that increased electrical driving force resulted in higher alanine transport activity of the mutant transporter relative to wild-type SNAT2. Because Na^+ binding to SNATs from the extracellular side was proposed to be one of the major voltage-dependent steps in the transport cycle (14), the possibility has to be considered that the mutations in position N82A interfere with Na^+ activation of amino acid transport, as described in the next paragraphs.

Mutations at Asn^{82} *Inhibit Na*$^+$*-dependent Anion Leak Currents*—SNAT2 is associated with an uncoupled anion conductance that is activated by Na^+ binding to SNAT2 but inhibited by the binding of transported amino acid substrates (20). We used this anion conductance as an assay to test the kinetics of interaction of Na^+ with the mutant transporters. At negative voltages, application of 10 mM alanine to $SNAT2_{WT}$ inhibited a tonic anion current caused by outflow of intracellular SCN^-, resulting in an apparent outward current (the average value was 360 ± 130 pA at −90 mV; Fig. 4, *C* and *D*, $n = 5$). In contrast, application of 10 mM alanine to $SNAT2_{N82A}$ did not inhibit SCN^- outflow current (Fig. 4, *A* and *D*, $n = 6$). $SNAT2_{N82S}$ showed intermediate behavior with small inhibition of anion current at −90 mV (66 ± 9 pA; Fig. 4, *B* and *D*, $n = 4$).

The results described in the previous paragraph suggest that the Asn^{82} mutations either interfere with the ability of SNAT2 to mediate anion current and/or that the Na^+ concentration is too low to activate anion current. To differentiate between these possibilities, we determined whether application of higher concentrations of extracellular Na^+ could activate anion current in $SNAT2_{N82A}$- and $SNAT2_{N82S}$-expressing cells (in the presence of 140 mM intracellular KSCN). For $SNAT2_{WT}$, 140 mM Na^+ mediated large inward currents upon switching from Na^+-free extracellular solution (*N*-methylglucamine replacement) to 140 mM Na^+ (Fig. 5*A*) in the absence of extracellular amino acid (−98 ± 16 pA, $n = 5$; Fig. 5*B*). In contrast, $SNAT2_{N82A}$-transfected cells showed only small anion current responses to $[Na^+]$ jumps at the same conditions (23 ± 5 pA, $n = 6$; Fig. 5, *A* and *B*). These anion currents were not significantly larger than the ones recorded from non-

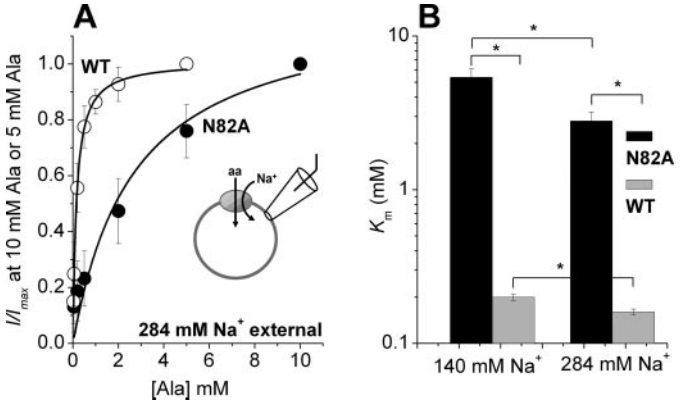

FIGURE 6. **The reduction of alanine affinity by the N82A mutation can be overcome by increasing extracellular [Na^+].** *A*, the apparent affinity of $SNAT2_{N82A}$ and $SNAT2_{WT}$ for alanine was determined by recording substrate-induced transport current as a function of [alanine] in the presence of 284 mM extracellular NaMes at 0 mV. The maximum currents before normalization were 81 ± 15 pA (*WT*) and 25 ± 15 pA (N82A). *B*, comparison of the apparent affinity for L-alanine of $SNAT2_{N82A}$ and $SNAT2_{WT}$ in the presence of 140 and 284 mM extracellular Na^+. Two-way ANOVA indicates significant difference between the K_m values for $SNAT2_{WT}$ and N82A, as well as significant difference between the K_m values at 140 and 284 mM [Na^+] (at the $p < 0.05$ level, indicated by the *asterisks*.

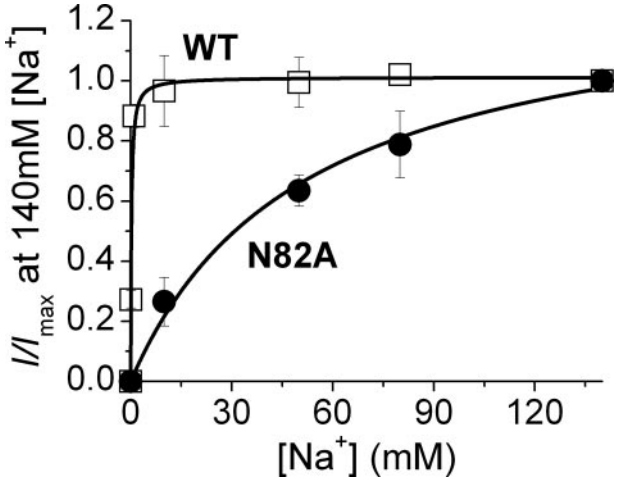

FIGURE 7. **The N82A mutation results in a dramatic reduction of the apparent SNAT2 affinity for Na^+.** The apparent affinities of $SNAT2_{N82A}$ (*circles*) and $SNAT2_{WT}$ (*squares*) for extracellular Na^+ were measured by recording 20 mM L-alanine-induced transport current as a function of extracellular [Na^+] at a membrane potential of −60 mV. Before normalization, which was used to illustrate the dramatic differences in K_{Na^+}, the I_{max} of $SNAT2_{N82A}$ was 10 ± 3% of that of $SNAT2_{WT}$. *WT*, wild type.

transfected control cells (18 ± 2 pA, $n = 5$; Fig. 5, *A* and *B*). $SNAT2_{N82S}$ showed Na^+-induced anion current (-36 ± 4 pA, $n = 8$), although it was significantly smaller compared with $SNAT2_{WT}$ (Fig. 5*B*). For $SNAT2_{WT}$ this anion current was Na^+ concentration-dependent, saturating with an apparent K_m for Na^+ (K_{Na^+}) of 100 ± 7 mM ($n = 5$; Fig. 5*G*). In contrast, even at the highest Na^+ concentration used (300 mM), $SNAT2_{N82A}$ anion current was less than 2-fold that of nontransfected control cells (Fig. 5*C*). This small anion current prevented us from estimating the K_{Na^+} of this mutant transporter for Na^+. However, SNAT2 with the more conservative mutation N82S clearly showed a [Na^+]-dependent anion current with a K_{Na^+} value of about 300 mM (Fig. 5*D*; $n = 8$), 3-fold higher than that of wild-type SNAT2. An increase of K_{Na^+} was also observed for $SNAT2_{Y337A}$, whereas the R374Q mutation showed a K_{Na^+} similar to wild-type SNAT2 (Fig. 5, *E* and *F*). Together, these results suggest that mutations to position N82A interfere with the abilities of the transporter to interact with Na^+ and/or to mediate anion current.

Previously, we characterized a transporter with the H304A mutation that has a dramatically increased anion conductance but similar Na^+ activation kinetics of the anion current as the wild-type transporter (20). Therefore, we used the $SNAT2_{H304A,N82A}$ double mutant to test whether the anion conductance of $SNAT2_{N82A}$ could be restored by the additional introduction of the H304A mutation. We measured the leak anion current activated by extracellular Na^+ for the double mutant transporter in the presence of 140 mM intracellular KSCN without extracellular alanine. Application of 140 mM Na^+ induced a large inward leak anion current for $SNAT2_{H304A}$ at 0 mV (Fig. 6; −340 ± 120 pA, $n = 6$). This leak anion current was 6-fold larger than that of $SNAT2_{WT}$ (−98 ± 16 pA, $n = 5$; Fig. 5*B*). 140 mM Na^+ induced much smaller leak anion currents (−34 ± 14 pA, $n = 5$; supplemental Fig. S4, *A* and *B*) in $SNAT2_{H304A,N82A}$, which were on average 2-fold larger than those in nontransfected cells (−18 ± 2 pA, $n = 5$), indicating that at least some of the ability of SNAT2 to carry anion current was restored by the double mutant. Kinetic analysis showed that anion current induced by Na^+ began to saturate at high [Na^+] with an apparent K_{Na^+} of 175 ± 37 mM ($n = 5$) for $SNAT2_{H304A}$ (supplemental Fig. S4*C*), which was only slightly increased compared with $SNAT2_{WT}$ ($K_{Na^+} = 100 \pm 7$ mM, $n = 5$; Fig. 5*G*). In contrast, the small anion current induced by Na^+ in $SNAT2_{H304A,N82A}$ increased linearly with increasing [Na^+], suggesting that Na^+ was not able to saturate its binding site on the double mutant transporter, even at a [Na^+] of 300 mM. This result indicates that the N82A mutation prevents $SNAT2_{H304A}$ from interacting with Na^+ with a low K_{Na^+}.

The N82A Mutation Interferes with the Interaction of SNAT2 with Na^+—Amino acid and the cotransported Na^+ ion were proposed to bind to SNATs from the extracellular side in an ordered sequence, with Na^+ binding first and amino acid binding second (14). If this is the case, then defective Na^+ binding to a mutant transporter with a high K_{Na^+} should also result in a high apparent K_m for alanine binding as well, according to Equation 1.

$$K_m = K_{aa} \cdot \left(\frac{K_{Na^+} + [Na^+]}{[Na^+]} \right) \qquad \text{(Eq. 1)}$$

Here, K_{aa} = the intrinsic dissociation constant of SNAT2 for amino acid. For wild-type SNAT2 the K_m for alanine was reduced by only a factor of 1.29 when doubling [Na^+] from 140 mM ($K_m = 200 \pm 20$ μM) to 284 mM ($K_m = 155 \pm 10$ μM; Fig. 6), as expected from Equation 1 with a K_{Na} of 100 mM and K_{aa} of 119 μM. In contrast, doubling [Na^+] resulted in a 2-fold reduction of the apparent K_m of $SNAT2_{N82A}$ for alanine (2.7 ± 0.4 mM at 284 mM extracellular [Na^+]; Fig. 6), suggesting a K_{aa} of 80 μM and a K_{Na^+} of 10 M from Equation 1 (see Fig. 6*B* for statistical analysis).

To measure the K_{Na^+} of wild-type and mutant SNAT2 more directly, we measured alanine-induced transport current as a function of extracellular [Na^+] (Fig. 7). This was

done at a membrane potential of −60 mV, at which $SNAT2_{N82A}$ generates small but measurable transport current, and at [alanine] of 20 mM. Under these conditions, the apparent K_{Na^+} of $SNAT2_{WT}$ was 230 ± 40 μM (alanine-bound transporter, $n = 5$), whereas the K_{Na^+} of $SNAT2_{N82A}$ was increased 230-fold to 52 ± 14 mM (Fig. 7, $n = 5$). These results directly show that the N82A mutation dramatically interferes with the ability of SNAT2 to interact with the sodium ion.

The N82A Mutation Eliminates Transient Charge Movement in Response to Voltage Jumps—In the absence of amino acid substrate, SNATs respond with transient currents to step changes of the transmembrane potential. For SNAT1, these transient currents were dependent on the Na^+ concentration (14). Thus, they were proposed to be caused by Na^+ association with SNAT1 and/or voltage-dependent reorientation of the empty transporter, in analogy to other Na^+-coupled, secondary active transporters (25–29). Consistent with this proposal, $SNAT2_{WT}$ expressed in HEK293 cells responded to voltage jumps from a holding potential of 0 mV to a range of potentials from −150 to + 90 mV (see voltage protocol in Fig. 8*A*) with transient, alanine-sensitive currents that were manifested as an initial transient component that precedes steady-state alanine-induced transport current (Fig. 8*A*, *bottom panel*). Within the Na^+ concentration range tested, the maximum charge obtained from extrapolating to membrane potentials that saturated the charge movement was independent of [Na^+] (Fig. 8*B*), suggesting that most of the charge movement is caused by Na^+ binding but not by reorientation of the empty transporter. If reorientation of the empty transporter would contribute to the charge movement, it would be expected that this maximum charge changes at low [Na^+], as more transporters populate the Na^+-free states. In addition, K_{Na^+} was voltage-dependent, decreasing 4-fold while changing V_m from 0 mV to −60 mV (data not shown), further supporting the idea of voltage-dependent Na^+ binding to SNAT2.

The charge movements, *Q*, of the on and the off response of these currents were similar to each other, within experimental error (Fig. 8*C*), suggesting that this charge movement is capacitive in nature. The voltage jump-induced charge movement was voltage-dependent and could be fit with a Boltzmann-like relationship with an apparent valence, z_Q, of 0.55 ± 0.28 ($n = 4$), and a midpoint potential, $V_{½}$, of −16 ± 10 mV ($n = 4$; Fig. 8*D*, *bottom panel*). Charge movements in response to voltage jumps were absent in nontransfected control cells (Fig. 8*A*, *second panel* from the *top*). In contrast to $SNAT2_{WT}$, no alanine-sensitive charge movement was seen in $SNAT2_{N82A}$-transfected cells (Fig. 8*D*, *middle panel*) after jumping the voltage from 0 mV to positive potentials. Only little inward charge movement was observed after voltage jumps to membrane potentials more negative than −30 mV. These results are consistent with the idea that at 140 mM and at voltages more positive than −30 mV, only a little Na^+ is bound to $SNAT2_{N82A}$ because of its high K_{Na^+}, thus leading to reduced Na^+-dependent charge movement and reduced amino acid transport activity. Although unlikely in light of the high K_{Na^+} and because the N82A mutation does not alter the net charge of the transporter, an alternative explanation for the absence of voltage jump-induced charge movement is that Na^+ binding is electroneutral in the mutant transporter, but not in wild-type SNAT2.

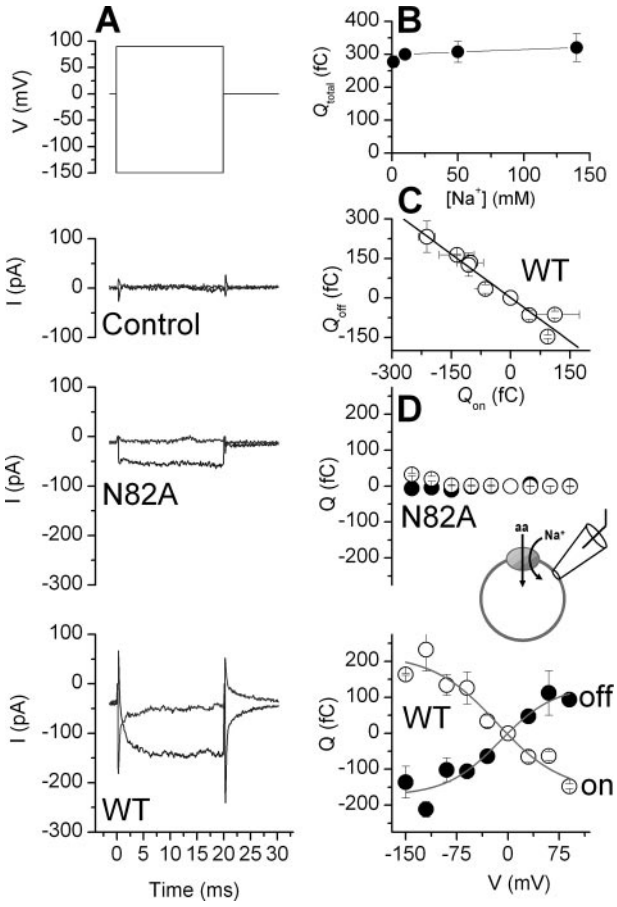

FIGURE 8. **Voltage jump-induced transient currents are absent in $SNAT2_{N82A}$.** *A*, the voltage jump protocol shown in the *top panel* was used to measure alanine-sensitive (10 mM for $SNAT2_{WT}$ and nontransfected cells, 20 mM for $SNAT2_{N82A}$) transport and transient currents (140 mM extracellular NaMes and 140 mM intracellular KMes.). *B*, the maximum charge movement (Q_{total}) is independent of extracellular [Na^+]. Q_{total} was obtained from extrapolating the Boltzmann-type *Q-V* dependence to saturating values at both positive and negative voltage extremes (see also Fig. 8*D*). *C*, the total charge, *Q*, moved in the off-response equals that in the on-response in $SNAT2_{WT}$-expressing cells (*Q* was determined by integrating the transient part of the current response). *D*, voltage dependence of the charge moved in the on response and off response in $SNAT2_{N82A}$- (*top panel*) and $SNAT2_{WT}$- (*bottom panel*) expressing cells. The *solid lines* represent a fit of the data with a Boltzmann relationship. *WT*, wild type.

DISCUSSION

Here we have studied the functional effects of mutations of three highly conserved amino acid residues in the putative TMDs 1, 7, and 8 of SNAT2, which is widely expressed in mammalian tissue and responsible for Na^+-driven transport of glutamine, alanine, and other small, neutral amino acids (5, 8, 12, 13). The main result of this study is that mutations to Asn^{82} dramatically increase the K_{Na^+} for interaction of the transporter with the sodium ion. Although the experimental K_{Na^+} reflects the *apparent* Na^+ affinity, which is also determined by other steps in the transport cycle, such as substrate binding affinity, we interpret this increased K_{Na^+} as dramatically decreased *intrinsic* Na^+ affinity of $SNAT2_{N82A}$. Therefore, we conclude that the N82A mutation virtually eliminates the inter-

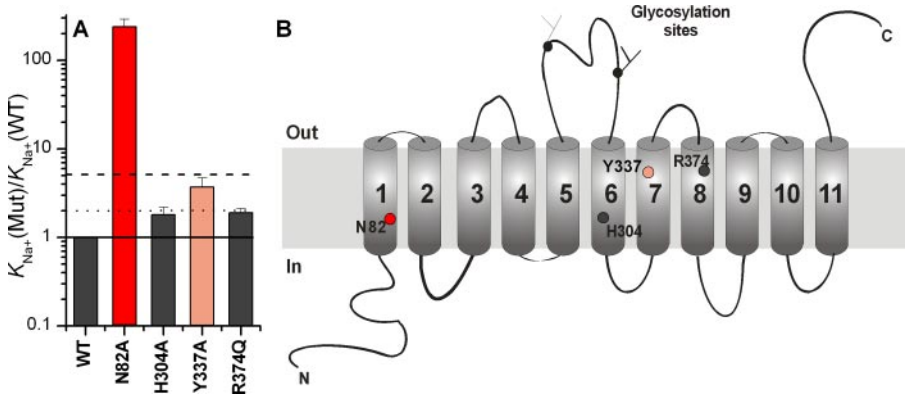

FIGURE 9. **Mapping of the effect of mutations on the K_{Na^+} (*A*) onto the predicted transmembrane topology of SNAT2 (*B*).** The mutations showing a >5-fold effect on K_{Na^+} (K_{Na^+}(Mut)/K_{Na^+}(WT) > 5) are color-coded in *red*, those with 2 < K_{Na^+}(Mut)/K_{Na^+} (WT) < 5 are color-coded in *salmon*, and mutations with <2-fold effect on K_{Na^+} are shown in *gray*.

action of the transporter with Na^+ at physiological conditions, whereas a mutation in position 337 also inhibited Na^+ binding but to a much smaller extent (summarized in Fig. 9*A*). This result suggests that the conserved amino acid residue asparagine 82 in TMD1 of SNAT2 is required for Na^+ interaction and amino acid transport by SNAT2. At physiological ion concentrations (140 mM extracellular Na^+), the binding site of the mutant transporter for Na^+ is far from being saturated, thus impeding amino acid binding and transport. However, even when raising [Na^+] to saturating levels, amino acid transport activity is only partially restored, indicating that the mutation also impairs the conformational changes that are most likely accompanying transport. Our results are consistent with a recent report showing that mutation of the amino acid analogous to Asn^{82} in SNAT3 (Asn^{76}) to histidine impairs amino acid transport, although Schneider *et al.* (24) did not elaborate on the underlying molecular cause(s) for this inhibition. The results presented here suggest that the N76H mutation inhibits amino acid transport by SNAT3 by also interfering with its ability to interact with Na^+, indicating similar interaction mechanisms of the two transporters with Na^+.

One attractive possibility to consider is that the asparagine side chain in position 82 contributes directly to the coordination of Na^+ by SNAT2. This idea is supported by the virtual elimination of Na^+ interaction with the empty transporter by the N82A mutation, whereas the more conservative N82S mutation still allows Na^+ to associate with the transporter, albeit with considerable lower apparent affinity than wild-type SNAT2. In contrast to the methyl side chain of alanine, the hydroxyl oxygen of serine may be able to partially replace the amide oxygen of asparagine for contributing to the coordination of the bound Na^+. However, even if the Asn^{82} side chain is directly involved in coordinating Na^+, other amino acid residues contributing to this coordination are likely to be found in future studies, because Na^+ prefers to be coordinated in proteins by six ligands (30).

Our data do not rule out indirect effects of the mutations that reduce Na^+ affinity through a long range effect. Such indirect effects are inherent in the mutagenesis approach. However, two types of indirect effects of the mutations are unlikely: 1) mutations in position 82 do not result in a complete misfolding of SNAT2 because the general binding sites for amino acid and Na^+ are preserved, although they bind their substrate with dramatically reduced apparent affinity; and 2) indirect effects caused by the coupling of individual reaction steps in the transport cycle are unlikely because our approach is based on the study of these individual steps in isolation.

SNAT1 was shown to be able to bind Na^+ in the absence of amino acid (14), and a similar observation was recently made for SNAT2 (20). This suggests a sequence of events in which Na^+ associates with SNAT2 first, followed by the binding of amino acid. Thus, the fractional occupation of the Na^+-binding site should have a direct effect on the K_m of the transporter for amino acid (Equation 1). Consistently, we find that $SNAT2_{N82A}$ has a dramatically increased K_m for alanine compared with wild-type $SNAT2_{WT}$. As stated above, we interpret this increase in K_m as a reduction in the apparent substrate affinity. This alanine affinity increases when raising [Na^+] to a larger extent in the mutant transporter than in $SNAT2_{WT}$ (Fig. 7). Therefore, we propose that the low apparent alanine affinity of the mutant transporters is indirectly caused by their low affinity for Na^+, which reduces the fractional occupation of the Na^+-binding site at 140 mM Na^+, in turn resulting in a high K_m for alanine. Consistently, our results suggest that the actual dissociation constant for amino acid, which reflects the intrinsic, not the apparent affinity, is 80 μM in $SNAT2_{N82A}$ (Equation 1). This value is not significantly different from the wild-type value (119 μM).

SNAT2 belongs to the SLC38 family of transport proteins, which is part of a larger superfamily of transporters that also includes the vesicular amino acid transporters, SLC32 (31), proton-driven amino acid transporters, SLC36 (32), and plant amino acid permeases (33). It was also suggested that the bacterial amino acid/polyamine/organocation family is evolutionarily distantly related to the SLC38 transporters (34). The transporters of the superfamily have 10–14 predicted transmembrane domains, with TMD1 showing an extraordinary high degree of conservation within the subfamilies. This observation fits well with our data, showing that a highly conserved amino acid residue in TMD1 of SNAT2 is involved in cation coupling of amino acid transport, as illustrated by the mapping of the effect of the mutations studied here onto the predicted transmembrane topology model of SNAT2 (Fig. 9*B*). This result may indicate that TMD1 is a critical component of the transport pathway, consistent with previous reports on plant amino acid transporters (35) and an amino acid/polyamine/organocation family member (36) showing that mutations to amino acid in putative TMD1 inhibit amino acid transport. Together, these results point to a functional importance of TMD1 for amino acid transport by SNAT2 and provide a framework for future structure function studies on SLC38 transporters that should involve residues in TMD1.

In contrast to Asn^{82}, the polar amino acid residue Arg^{374}, which is also highly conserved among the SLC38 members, appears to not be critical for amino acid transport and Na^+ interaction. In the predicted transmembrane topology of SLC38 transporters (Fig. 9*B*), Arg^{374} and His^{304} are the only amino acid residues with potential charge. Because our mutagenesis results suggest that positive charge in position 374, as well as 304 (20), is not required for transport activity, it is unlikely that the SLC38 transporters utilize charge from amino acid side chains to compensate for charges of the zwitterionic amino acid or the cotransported Na^+ ion. It can be speculated that SNAT2 rather uses partial charges from local dipoles or helix dipoles for charge compensation.

In conclusion, this work demonstrates the functional importance of the highly conserved aspargine residue in position 82. Mutations to this position result in impaired amino acid transport, as well as in a dramatic defect of the interaction of SNAT2 with the cotransported sodium ion. Our results highlight the importance of predicted TMD1 for the function of SLC38 transporters and those of related families.

Acknowledgment—We thank Dr. Diez-Sampedro for help with the MeAIB uptake studies and for critical reading of the manuscript.

REFERENCES

1. Bode, B. P. (2001) *J. Nutr.* **131,** 2475S–2485S
2. Daikhin, Y., and Yudkoff, M. (2000) *J. Nutr.* **130,** 1026–1031
3. Young, V. R., and Ajami, A. M. (2001) *J. Nutr.* **131,** 2449S–2459S
4. Wang, H., Huang, W., Sugawara, M., Devoe, L. D., Leibach, F. H., Prasad, P. D., and Ganapathy, V. (2000) *Biochem. Biophys. Res. Commun.* **273,** 1175–1179
5. Varoqui, H., Zhu, H., Yao, D., Ming, H., and Erickson, J. D. (2000) *J. Biol. Chem.* **275,** 4049–4054
6. Sugawara, M., Nakanishi, T., Fei, Y. J., Huang, W., Ganapathy, M. E., Leibach, F. H., and Ganapathy, V. (2000) *J. Biol. Chem.* **275,** 16473–16477
7. Chaudhry, F. A., Reimer, R. J., Krizaj, D., Barber, D., Storm-Mathisen, J., Copenhagen, D. R., and Edwards, R. H. (1999) *Cell* **99,** 769–780
8. Hatanaka, T., Huang, W., Wang, H., Sugawara, M., Prasad, P. D., Leibach, F. H., and Ganapathy, V. (2000) *Biochim. Biophys. Acta* **1467,** 1–6
9. Fei, Y. J., Sugawara, M., Nakanishi, T., Huang, W., Wang, H., Prasad, P. D., Leibach, F. H., and Ganapathy, V. (2000) *J. Biol. Chem.* **275,** 23707–23717
10. Sugawara, M., Nakanishi, T., Fei, Y. J., Martindale, R. G., Ganapathy, M. E., Leibach, F. H., and Ganapathy, V. (2000) *Biochim. Biophys. Acta* **1509,** 7–13
11. Nakanishi, T., Sugawara, M., Huang, W., Martinedale, R. G., Leibach, F. H., Ganapathy, M. E., Prasad, P. D., and Ganapathy, V. (2001) *Biochem. Biophys. Res. Commun.* **281,** 1343–1348
12. Yao, D., Mackenzie, B., Ming, H., Varoqui, H., Zhu, H., Hediger, M. A., and Erickson, J. D. (2000) *J. Biol. Chem.* **275,** 22790–22797
13. Mackenzie, B., and Erickson, J. D. (2004) *Pfluegers Arch. Eur. J. Physiol.* **447,** 784–795
14. Mackenzie, B., Schafer, M. K., Erickson, J. D., Hediger, M. A., Weihe, E., and Varoqui, H. (2003) *J. Biol. Chem.* **278,** 23720–23730
15. Reimer, R. J., Chaudhry, F. A., Gray, A. T., and Edwards, R. H. (2000) *Proc. Natl. Acad. Sci. U. S. A.* **97,** 7715–7720
16. Chaudhry, F. A., Schmitz, D., Reimer, R. J., Larsson, P., Gray, A. T., Nicoll, R., Kavanaugh, M., and Edwards, R. H. (2002) *J. Neurosci.* **22,** 62–72
17. Hertz, L. (1979) *Prog. Neurobiol.* **13,** 277–323
18. Jauch, P., Petersen, O. H., Lauger, P., Jauch, P., and Lauger, P. (1986) *J. Membr. Biol.* **94,** 99–115
19. Jauch, P., and Lauger, P. (1986) *J. Membr. Biol.* **94,** 117–127
20. Zhang, Z., and Grewer, C. (2007) *Biophys. J.* **92,** 2621–2632
21. Zhang, Y., and Kanner, B. I. (1999) *Proc. Natl. Acad. Sci. U. S. A.* **96,** 1710–1715
22. Bismuth, Y., Kavanaugh, M. P., and Kanner, B. I. (1997) *J. Biol. Chem.* **272,** 16096–16102
23. Grewer, C., Watzke, N., Wiessner, M., and Rauen, T. (2000) *Proc. Natl. Acad. Sci. U. S. A.* **97,** 9706–9711
24. Schneider, H.-P., Broer, S., Broer, A., and Deitmer, J. W. (2007) *J. Biol. Chem.* **282,** 3788–3798
25. Loo, D., Hazama, A., Supplisson, S., Turk, E., and Wright, E. (1993) *Proc. Natl. Acad. Sci. U. S. A.* **90,** 5767–5771
26. Lu, C. C., and Hilgemann, D. W. (1999) *J. Gen. Physiol.* **114,** 445–457
27. Wadiche, J. I., Arriza, J. L., Amara, S. G., and Kavanaugh, M. P. (1995) *Neuron* **14,** 1019–1027
28. Watzke, N., Bamberg, E., and Grewer, C. (2001) *J. Gen. Physiol.* **117,** 547–562
29. Zhou, Y., and Kanner, B. I. (2005) *J. Biol. Chem.* **280,** 20316–20324
30. Page, M. J., and Di Cera, E. (2006) *Physiol. Rev.* **86,** 1049–1092
31. McIntire, S. L., Reimer, R. J., Schuske, K., Edwards, R. H., and Jorgensen, E. M. (1997) *Nature* **389,** 870–876
32. Boll, M., Daniel, H., and Gasnier, B. (2004) *Pfluegers Arch. Eur. J. Physiol.* **447,** 776–779
33. Young, G. B., Jack, D. L., Smith, D. W., and Saier, M. H., Jr. (1999) *Biochim. Biophys. Acta* **1415,** 306–322
34. Jack, D. L., Paulsen, I. T., and Saier, M. H. (2000) *Microbiology* **146,** 1797–1814
35. Ortiz-Lopez, A., Chang, H., and Bush, D. R. (2000) *Biochim. Biophys. Acta* **1465,** 275–280
36. Pi, J., Chow, H., and Pittard, A. J. (2002) *J. Bacteriol.* **184,** 5842–5847